BMC Medical Imaging

RESEARCH

Open Access

A comparative study of different types of connective tissue-associated interstitial lung disease

Xinyi Li[1], Hongmei Zhang[1], Xiaoyue Zhang[1], Guokun Wang[1], Xue Zhao[1] and Jinling Zhang[1*]

Abstract

Introduction Interstitial lung disease (ILD) is an important pulmonary complication of connective tissue disease (CTD). This study aimed to analyze high-resolution computed tomography (HRCT) manifestations of different connective tissue-associated interstitial lung diseases (CTD-ILDs) to improve diagnostic accuracy.

Method This study retrospectively included 99 patients diagnosed with CTD-ILD between September 2017 and July 2024. Visual assessment and quantitative CT analysis were used to evaluate HRCT manifestations.

Results The age of the rheumatoid arthritis (RA) group was significantly greater than that of the polymyositis/dermatomyositis (PM/DM) and systemic sclerosis (SSc) groups ($p=0.025$ and $p=0.02$), with a mean age of 64.4 ± 10 years. The most common HRCT pattern of CTD-ILD was nonspecific interstitial pneumonia (NSIP) ($p=0.008$); the adjusted residual > 1.96, usual interstitial pneumonia (UIP) was most frequently observed in the RA group, organizing pneumonia (OP) was most commonly observed in the PM/DM group, and lymphocytic interstitial pneumonia (LIP) was observed only in the primary Sjögren's syndrome (pSjS) group. The CTD-ILD groups exhibited significant differences in bronchiectasis ($\chi2=11.256$, $p=0.0022$), esophageal dilatation ($\chi2=33.923$, $p<0.001$), mediastinal lymph node enlargement ($\chi2=10.103$, $p=0.041$), and thin-walled cysts ($\chi2=14.081$, $p=0.006$). Adjusted residual > 1.96, esophageal dilatation was commonly observed in the SSc group; bronchiectasis was more common in the RA group; mediastinal lymph node was more common in the pSjS group. Statistically significant differences in the predominance of different CTD-ILDs ($\chi2=20.814$, $p=0.0046$). The PM/DM group exhibited significant consolidation and reticulation. The extensive honeycombing was present in the RA-ILD group ($p=0.044$). Based on logistic binary regression analysis, bronchial dilatation (odds ratio: 4.506, $p=0.005$) and extensive honeycombing (odds ratio: 1.282, $p=0.021$) were significant predictors of RA-ILD, while lymph node enlargement (odds ratio: 3.314, $p=0.039$) and thin-walled cysts (odds ratio: 6.278, $p=0.001$) were predictors of pSjS-ILD.

Conclusion Different types of CTD-ILD have characteristic HRCT manifestations.

Clinical trial number As this study involved standard clinical procedures and assessments without an experimental treatment protocol, it did not require registration with a public clinical trials registry.

Keywords Interstitial lung disease, Connective tissue diseases, Quantitative CT, Radiology

*Correspondence:
Jinling Zhang
jinlingzi@163.com
[1]Department of CT, The Second Affiliated Hospital of Harbin Medical University, Harbin 15000, China

Introduction

Connective tissue disease (CTD) is a group of autoimmune disorders that are characterized by multisystem and multiorgan involvement, including rheumatoid arthritis (RA), polymyositis/dermatomyositis (PM/DM), systemic lupus erythematosus (SLE), systemic sclerosis (SSc), and primary Sjögren's syndrome (pSjS), among others. Pulmonary manifestations, often presenting as interstitial lung disease (ILD), are significant factors in CTD morbidity and mortality. These pulmonary manifestations can serve as initial indicators of CTD in patients and can occur prior to the development of typical clinical symptoms. A study reported that 19% of patients who were initially diagnosed with idiopathic interstitial pneumonia (IIP) developed CTD, highlighting the importance of early diagnosis [1]. Owing to its similarity to IIP, CTD-ILD can be classified according to the IIP classification system, which includes usual interstitial pneumonia (UIP), nonspecific interstitial pneumonia (NSIP), organizing pneumonia (OP), and lymphocytic interstitial pneumonia (LIP), among others [2]. Unfortunately, the invasive nature of lung biopsy often precludes the acquisition of pathological tissue samples. However, high-resolution computed tomography (HRCT) patterns are closely correlated with histopathological findings, making it an essential tool for providing anatomical information about lung lesions [3]. The presence and pattern of these findings play crucial roles in guiding treatment decisions and determining patient prognosis. Previous studies have shown that the heterogeneity of CTD-ILDs is high, and it cannot be studied as a whole; thus, it is necessary to categorize CTD-ILDs for research. In this study, we used CTD-ILD types as the classification criteria to explore the differences in imaging performance for different types of CTD-ILD to provide guidance for precise clinical diagnosis and treatment [4].

Owing to its noninvasive nature and applicability to most patients, HRCT has become the primary tool for evaluating ILD. However, the interpretation of images by physicians may be subjective, leading to potential inaccuracies. In recent years, quantitative CT analysis has been widely accepted because of its objectivity and ability to reflect histologic features [5]. Nevertheless, the complexity of CTD-ILD imaging and the multisystemic nature of the disease make it challenging to comprehensively and accurately quantify all signs. Consequently, most previous studies have focused primarily on describing the signs of CTD-ILD on the basis of visual assessment alone. Therefore, this study aimed to analyze the HRCT manifestations of different CTD-ILD types by combining quantitative CT and visual assessment, thereby increasing diagnostic accuracy for various types of CTD-ILD.

Materials and methods

This retrospective study included 99 patients (34 patients with RA-ILD, 27 patients with pSjS-ILD, 16 patients with SSc-ILD, 16 patients with PM/DM-ILD, and 6 patients with SLE-ILD) who underwent chest HRCT and who were diagnosed through a multidisciplinary approach at the Second Affiliated Hospital of Harbin Medical University between September 2017 and July 2024. All the patients' CTD diagnoses conformed to the criteria established by the European League Against Rheumatism (EULAR) and the American College of Rheumatology (ACR). The study was approved by the hospital's ethics committee (Ethics No. YJSKY2024-057), and all the images and data were securely extracted from electronic records to maintain patient privacy confidentiality and ethical standards.

CT methods

In this study, a Philips 256-row Brilliance iCT scanner, which was manufactured by a Dutch company, was used to perform a CT scan at the end of the patient's maximal inspiration without contrast injection. The patient was scanned in a supine position, with the scan range extending from the lung base to the lung apex. The scanning parameters were as follows: layer thickness: 1 mm; layer spacing: 5 mm; voltage: 120 kV; pitch array: 512 × 512; and bone algorithm reconstruction. For lung window imaging, the window width was set to 1,500 HU, with a window level of -600 HU.

CT image processing and analysis

Visual assessment

All the CT images were independently evaluated in a randomized order by a physician with 8 years of experience who was not provided with any clinical information about the patients. The presence or absence of the following signs were recorded: (1) bronchiectasis; (2) esophageal dilatation; (3) mediastinal lymph node enlargement; (4) pleural effusion; (5) pulmonary artery widening; (6) pulmonary nodule; (7) honeycombing; (8) reticulation; (9) ground-glass opacity; (10) consolidation; 11. thin-walled cysts; and 12. pericardial effusion, where pulmonary artery widening was defined as a diameter of the main pulmonary artery ≥ 29 mm [6]. On the basis of the HRCT images, the predominant manifestations in each patient were identified and categorized into four groups: ground−glass opacity, reticulation, honeycombing, and consolidation. Determine the distribution of predominant manifestations, namely, along the bronchovascular bundles, subpleural or both. For each patient, a predominant HRCT pattern, including UIP, NSIP, OP, LIP, and others, was identified by the radiologist in consultation with the respiratory physician.

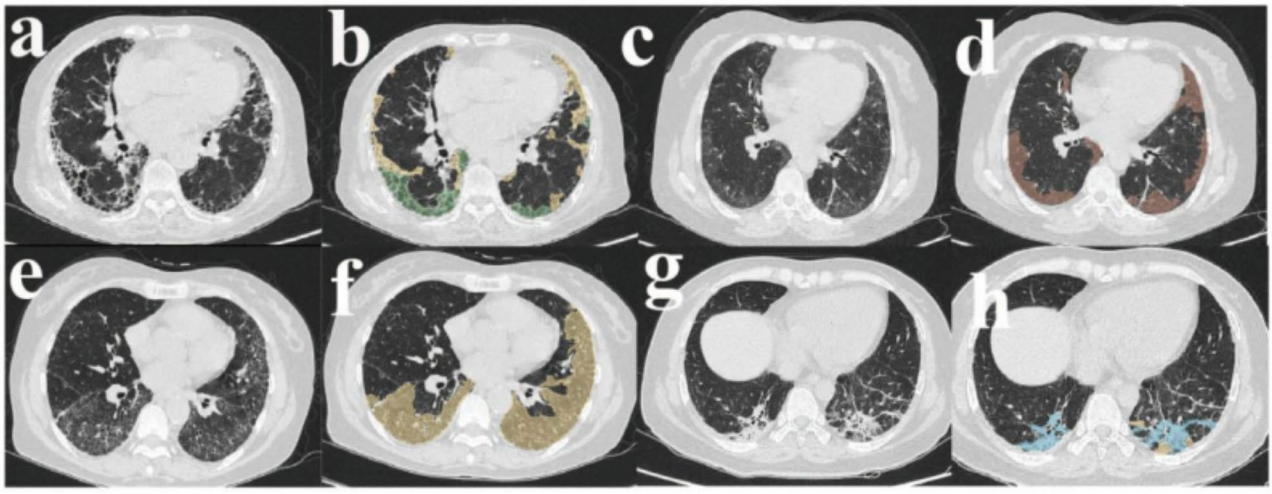

Fig. 1 **a**, **c**, **e**, and **g** are the original image without ROI labeling. **b**, **d**, **f**, and **h** are the original images labeled with ROIs, with different ROIs distinguished by different color zones: green for honeycombing; yellow for reticulation; red for ground-glass opacity; and blue for consolidation

Table 1 Basic clinical data of patients in the CTD groups

	RA-ILD($n=33$)	pSjS-ILD ($n=27$)	SSc-ILD ($n=16$)	PM/DM-ILD ($n=16$)	SLE-ILD ($n=6$)	p	Post-hoc test
Gender(male: female)	9: 25	6: 21	1: 15	2: 14	0: 6	0.355	
Age (average ± SD)	64.4 ± 10	60.4 ± 11	54.7 ± 11.2	55.3 ± 8.6	58.8 ± 9.5	0.01	1>3;1>4

RA-ILD: rheumatoid arthritis-related interstitial lung disease; pSjS-ILD: primary Sjögren's syndrome-related interstitial lung disease; SSc-ILD: systemic sclerosis-related interstitial lung disease; PM/DM-ILD: polymyositis/dermatomyositis-related interstitial lung disease; SLE-ILD: systemic lupus erythematosus-related interstitial lung disease

1: RA-ILD; 2:pSjS-ILD; 3:SSc-ILD; 4:PM/DM-ILD; 5:SLE-ILD

Quantitative assessment

To ensure the accuracy of region of interest (ROI) outlining, this study employed manual outlining rather than an automatic expansion tool. The process was performed by two radiologists: one with 2 years of experience applying the corresponding module of the open-source software 3D Slicer (version 5.6.2, https://www.slicer.org) for ROI outlining and another with 5 years of experience who reviewed and modified the ROIs. The outlining process included all image levels, and the types of ROIs included honeycombing, ground-glass opacity, reticulation, and consolidation, each marked with distinct colors. The corresponding module of the software automatically quantified the volume of each lesion in the patient's images and calculated the percentage of total lung volume represented by the different lesions (Fig. 1).

Statistical methods

The Shapiro–Wilk test was used to assess the normality of the data. Descriptive statistics are presented as the mean ± standard deviation for normally distributed data and as (p25, p75) for data that did not conform to a normal distribution. The ages of the patients followed a normal distribution, and comparisons between groups were conducted via ANOVA, followed by post hoc analyses. The χ^2 test was used to compare HRCT manifestations, HRCT manifestation types, patient gender, and distribution of predominant manifestations across groups. The ranges of honeycombing, reticulation, ground–glass opacity, and consolidation between groups were assessed via the Kruskal–Wallis test. A p value < 0.05 was considered to indicate a significant difference. Adjusted standardized residuals were calculated to identify the groups that contributed to the significant differences in CT findings. An adjusted standardized residual greater than 1.96 or less than − 1.96 indicated a group with a significantly higher or lower frequency, respectively. Between-group comparisons were conducted between the RA-ILD group and other CTD-ILD groups as well as between the pSjS-ILD group and other CTD-ILD groups. Binary logistic regression analysis was employed to identify the predictors of RA-ILD and pSjS-ILD. The inclusion criterion consisted of the aforementioned statistically significant indicators. All analyses were conducted via SPSS 27.0.

Result

Patient information

A total of 99 patients with CTD-ILD who were diagnosed by a multidisciplinary team were included, with data related to age and gender presented in Table 1. No significant differences were observed in the male-to-female ratio among the different disease groups; however, the

number of female patients significantly exceeded that of male patients, with females accounting for 81.8% of the total patient population. A significant difference in age was observed among patients in the different disease groups ($p = 0.01$). Post hoc tests revealed that the RA group was significantly older than the PM/DM group and the SSc group ($p = 0.025$, $p = 0.02$). The average age of the RA group was 64.4 ± 10 years, which was significantly greater than that of the PM/DM and SSc groups.

Distribution of HRCT patterns of different types of CTD-ILDs

Among the HRCT manifestations of CTD-ILDs, the most prevalent type was NSIP (55.6%) (Fig. 2a), followed by UIP (30.3%) (Fig. 2b). LIP (Fig. 2c) was rare, accounting for 4%. Comparisons between groups with different types of CTD-ILD revealed significant differences ($p < 0.05$). Comparisons within the RA-ILD group revealed that the UIP pattern was the most common pattern in RA-ILD patients and was statistically significant (adjusted residuals > 1.96), and the adjusted residuals for the OP type (Fig. 2d) in PM/DM-ILD patients were > 1.96; these results indicated that PM/DM was most common in CTD-ILD patients with the HRCT pattern of OP. In this study, the LIP pattern was present only in pSjS patients, and the presence of the LIP pattern was not observed in patients with any of the other CTD-ILDs. The results are presented in Table 2.

Comparative analysis of HRCT imaging signs, significant manifestations, range of manifestations in different CTD-ILD groups, distrubtion and logistic regression analysis

Figure 3 shows the various HRCT features of the CTD-ILDs. There was no statistically significant difference between the groups in the presence or absence of pleural effusion, pulmonary artery widening, pulmonary

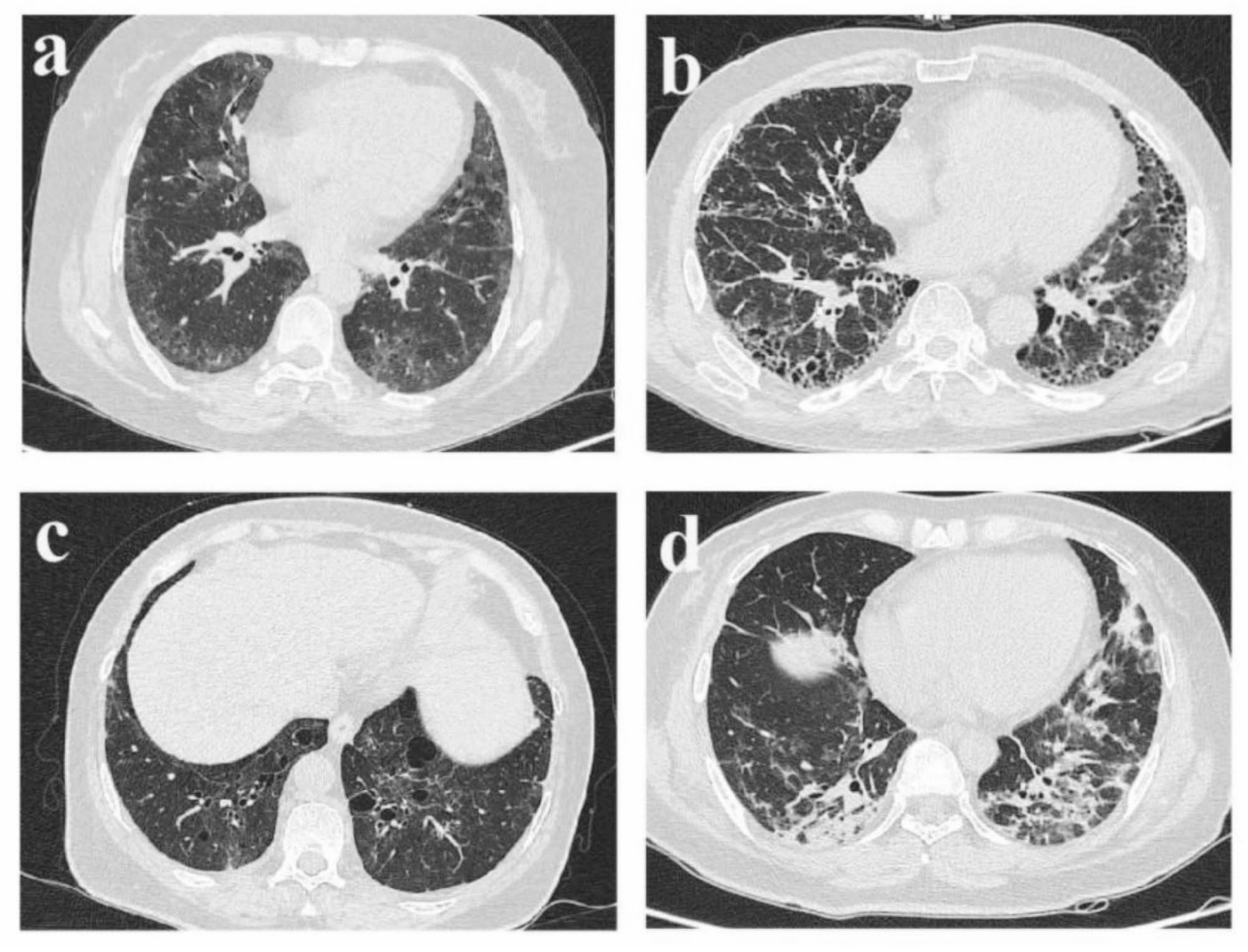

Fig. 2 **a**. An SSc patient with multiple reticulation and ground-glass opacity in both lungs, no obvious honeycombing, showing NSIP pattern. **b**. An RA patient with multiple areas of honeycombing and reticulation at the base of both lungs, showing a UIP pattern. **c**. A pSjS patient with multiple thin-walled cysts along vascular bundles in both lungs, accompanied by reticulation and ground-glass opacity, presenting as an LIP pattern. **d**. A PM patient with consolidation along the vascular bundles and subpleural distribution in both lungs, presenting as an OP pattern

Table 2 Distribution of HRCT patterns for different types of CTD-ILDs [n(%)]

	UIP	NSIP	LIP	OP	Others	x^2	*p*
RA-ILD(*n* = 34)	17(50)[a]	16(47.1)	0(0)	0(0)	1(2.9)	34.876	0.008
PSjS-ILD(*n* = 27)	6(22.2)	14(51.9)	4(14.8)[a]	1(3.7)	2(7.4)		
SLE-ILD(*n* = 6)	1(16.7)	4(66.7)	0(0)	1(16.7)	0(0)		
Ssc-ILD(*n* = 16)	4(25)	11(68.8)	0(0)	0(0)	1(6.3)		
PM/DM-ILD(*n* = 16)	2(12.5)	10(62.5)	0(0)	4(25)[a]	0(0)		
Total(*n* = 99)	30	55	4	6	4		

[a]: Significantly more frequent (adjusted standard residuals > 1.96)

[b]: Significantly less frequent (adjusted standard residuals <-1.96)

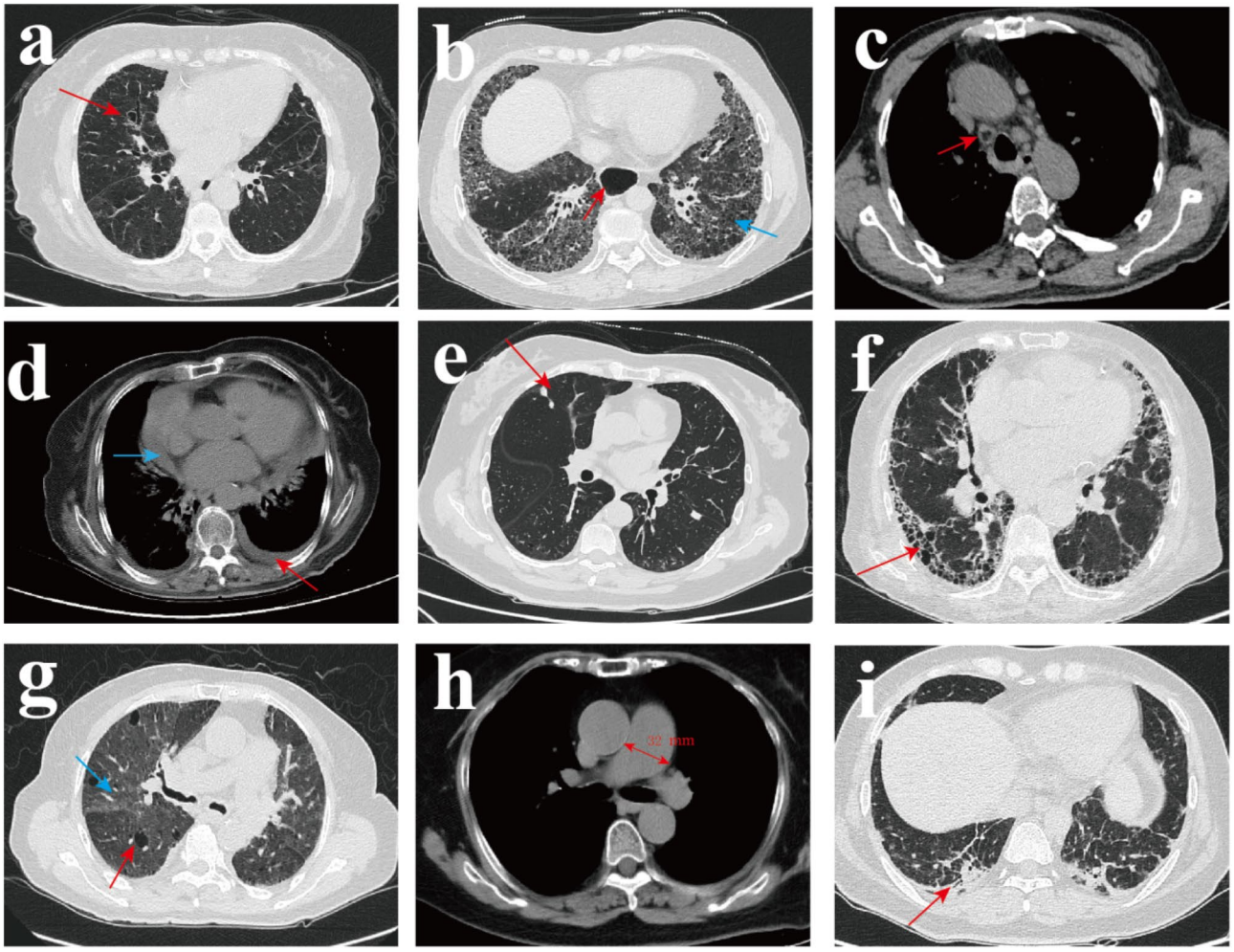

Fig. 3 **a**. bronchiectasis; **b**. esophageal dilatation(red arrow) and reticulation(blue arrow); **c**.mediastinal lymph node enlargement; **d**. pleural effusion(red arrow) and pericardial effusion(blue arrow); **e**. pulmonary nodule; **f**. honeycombing; **g**. thin-walled cysts(red arrow) and ground-glass opacity(blue arrow); **h**. pulmonary artery widening; **i**. consolidation

nodule, honeycombing, reticulation, ground-glass opacity, consolidation, or pericardial effusion. Different CTD-ILD groups exhibited significant differences in bronchiectasis ($\chi2 = 11.256$, $p = 0.0022$), esophageal dilatation ($\chi2 = 33.923$, $p < 0.001$), mediastinal lymph node enlargement ($\chi2 = 10.103$, $p = 0.041$), and thin-walled cysts ($\chi2 = 14.081$, $p = 0.006$). Bronchiectasis was most common in the RA-ILD group, and esophageal dilatation was mostly present in the SSc-ILD group. Mediastinal lymph node enlargement and thin-walled cysts were most common in the pSjS-ILD group. There was a significant difference in predominant manifestations between the groups ($\chi^2 = 20.814$, $p = 0.046$), with adjusted standardized residuals > 1.96, indicating that RA-ILD was the most common CTD, with honeycombing as the main type of presentation. PM/DM-ILD was

Table 3 Comparison of HRCT performance in different types of CTD-ILDs [n (%)]

HRCT performances	RA-ILD (*n* = 34)	pSjS-ILD (*n* = 27)	SSc-ILD (*n* = 16)	PM/DM-ILD (*n* = 16)	SLE-ILD (*n* = 6)	x^2	*p*
Bronchiectasis	24(70.6)[a]	12(44.4)	7(43.7)	5(31.3)	1(16.7)	11.256	0.022
Esophageal dilatation	2(5.9)[b]	1(3.7)[b]	10(62.5)[a]	1(6.3)	1(16.7)	33.923	<0.001
Mediastinal lymph node enlargement	14(41.2)	16(59.3)[a]	4(25)	3(18.8)	1(16.7)	10.103	0.041
Pleural effusion	2(5.9)	1(3.7)	1(6.3)	1(6.3)	1(16.7)	1.453	0.693
Pulmonary artery widening	7(20.6)	4(11.8)	6(17.6)	5(31.3)	2(33.3)	3.783	0.391
Pulmonary nodule	22(64.7)	22(81.5)[a]	8(50)	9(56.3)	4(66.7)	5.382	0.222
Honeycombing	20(58.8)[a]	11(40.7)	6(37.5)	3(18.8)[b]	2(12.5)	7.808	0.095
Reticulation	26(76.5)	20(74.1)	13(81.3)	14(87.5)	2(33.3)	7.395	0.157
Ground-glass opacity	23(67.6)	22(81.5)	11(68.8)	9(56.3)	4(66.7)	3.246	0.51
Consolidation	5(14.7)	8(29.6)	2(12.5)	5(31.3)	1(6.3)	3.771	0.43
Thin-walled cysts	11(32.4)	18(52.9)[a]	6(37.5)	2(12.5)[b]	2(33.3)	14.081	0.006
Pericardial effusion	6(17.6)	4(14.8)	2(12.5)	1(6.3)	3(50)[a]	6.48	0.241
Predominance						20.814	0.046
Ground-glass opacity	17(50)	12(44.4)	9(56.3)	4(25)	3(50)		
Reticulation	4(11.8)[b]	10(37)	3(18.8)	8(50)[a]	2(33.3)		
Honeycombing	13(38.2)[a]	4(14.8)	4(25)	2(12.5)	1(6.3)		
Consolidation	0(0)	1(3.7)	0(0)	2(12.5)[a]	0(0)		
Extent(p25,p75)							
Ground-glass opacity	(0,1.1)	(0.1,2.6)	(0,2)	(0,1.1)	(0,3.2)		0.783
Reticulation	(0.1,1)	(0,3.3)	(0.2,2.2)	(0.1,2.7)	(0,1.3)		0.253
Honeycombing	(0,4)	(0,1.6)	(0,1.7)	(0,0)	(0,0.5)		0.044
Consolidation	(0,0)	(0,0.1)	(0,0)	(0,0.3)	(0,1.4)		0.412
Distribution						8.950	0.345
PeriBVB	4(11.7)	6(22.2)	2(12.5)	3(18.8)	2(33.3)		
Subpleural	24(70.6)	11(40.7)[b]	11(68.6)	9(56.3)	4(66.7)		
PeriBVB + Subpl	6(17.6)	10(37)[a]	3(18.8)	4(25)	0(0)		

PeriBVB: Peri-bronchovascular; RA: rheumatoid arthritis-related interstitial lung disease; pSjS-ILD: primary Sjögren's syndrome-related interstitial lung disease; SSc-ILD: systemic sclerosis-related interstitial lung disease; PM/DM-ILD: polymyositis/dermatomyositis-related interstitial lung disease; SLE-ILD: systemic lupus erythematosus-related interstitial lung disease

[a]: Significantly more frequent (adjusted standard residuals > 1.96)

[b]: Significantly less frequent (adjusted standard residuals <-1.96)

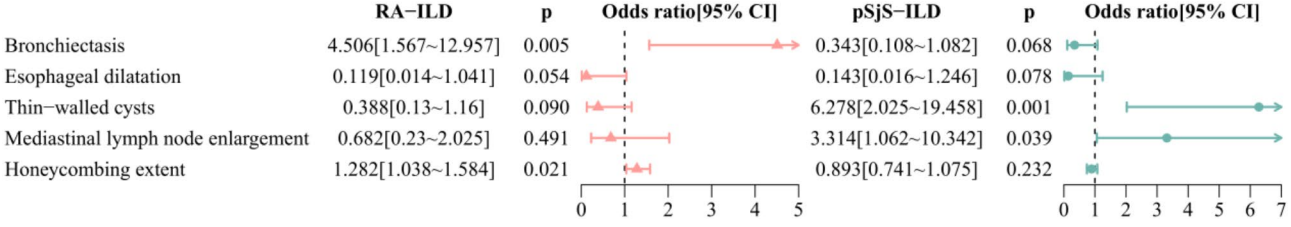

Fig. 4 Binary logistic regression analysis. RA-ILD: rheumatoid arthritis-related interstitial lung disease; pSjS-ILD: primary Sjögren's syndrome-related interstitiallung disease; 95%CI: 95% Confidence Interval

the most common CTD, with reticulation as the main type of presentation, and consolidation was similarly more common in the PM/DM-ILD group. With adjusted standardized residuals < -1.96, reticulation, which was the predominant presentation type, was less common in RA-ILD patients. The distribution of was not statistically significant, but there was a trend: distribution along the subpleura was more common in the RA group. The difference in the extent of honeycombing between the groups was statistically significant ($p = 0.044$), with RA-ILD patients showing more extensive honeycombing. The results are shown in Table 3. On the basis of the results of the binary logistic regression analysis of the RA-ILD and pSjS-ILD groups, significant predictors for both diseases were identified. Bronchiectasis (odds ratio: 4.506, $p = 0.005$) and the extent of honeycombing (odds ratio: 1.282, $p = 0.021$) were significant predictors of RA-ILD (Fig. 4). In contrast, pulmonary lymph node enlargement (odds ratio: 3.314, $p = 0.039$) and thin-walled cysts

(odds ratio: 6.278, $p = 0.001$) were identified as predictive factors for pSjS-ILD (Fig. 4).

Discussion

All types of CTD may be associated with ILD, with inflammatory processes arising from genetic, environmental, and autoimmune factors, leading to damage to the alveoli and pulmonary arteries [7]. One hypothesis posits that inflammation and epithelial damage stimulate an increase in fibroblasts and myofibroblasts, leading to extracellular matrix deposition and fibrosis [8–10]. Another hypothesis suggests that damage to alveolar cells induces the production of autoantibodies, thereby accelerating autoimmunity [11, 12]. This second hypothesis may explain why ILD often precedes the clinical manifestations of CTD. Pulmonary manifestations of certain CTDs may precede the onset of typical clinical symptoms by as much as five years [13], complicating diagnosis prior to the emergence of these hallmark signs. Some CTD-ILDs progress rapidly and may become life-threatening without timely treatment, as observed for PM/DM-ILD [14, 15]. Additionally, different types of CTD treatment, such as the application of steroids to treat SSc patients, may cause renal cortical crisis, but for the treatment of PM/DM-ILD or SLE-ILD, the early selection of appropriate means to improve patient treatment and prognosis is necessary. Selecting appropriate treatment methods as early as possible is essential for effective treatment [16]. Furthermore, patients may initially be evaluated by a general practitioner rather than a rheumatologist before the typical clinical symptoms manifest. In summary, it is essential to develop diagnostic methods that extend beyond traditional clinical symptoms and signs. Given the invasive nature of lung biopsies, HRCT has increasingly emerged as an effective alternative for the evaluation of CTD-ILD. Advances in technology have made quantitative CT imaging assessments more objective and precise. Owing to the multisystemic and complex nature of CTD, relying on quantitative assessments alone is challenging. In this study, we opted to combine visual assessment with quantitative CT, integrating the subjective expertise of human evaluators with the precision of technological tools to enhance the diagnosis of CTD-ILD.

In this study, NSIP was identified as the most prevalent pattern of CTD-ILD [17, 18], followed by UIP, which is consistent with previous findings [18]. Through intergroup comparisons, this study revealed a bias in the patterns associated with different CTD-ILDs. For example, individuals with RA exhibit a preference for the UIP pattern, possibly due to the more pronounced fibrotic changes associated with RA [18]. However, while UIP is often reported in RA patients, NSIP remains the predominant HRCT pattern, which may be attributed to diagnostic overlap with other CTDs, resulting in a higher frequency of the NSIP pattern [18]. OP is more prevalent among patients with PM/DM, whereas LIP is typically more common among patients with pSjS, which is consistent with previous research [13, 19]. Previous studies have indicated that SSc predominantly exhibits NSIP patterns, and this study revealed a similar trend [20]. However, the findings were not statistically significant, potentially due to the small sample size of SSc patients.

Previous studies have demonstrated a higher incidence of ILD in patients with RA. In a study that involved a nearly 20-year follow-up, 3% of patients developed ILD prior to the onset of RA, whereas 12% developed ILD during the follow-up period [21]. Furthermore, the literature indicates that ILD is a leading cause of increased mortality among RA patients [22]. A multicenter study on RA-ILD indicated that 9.4% of patients succumb to ILD as a direct consequence of the disease [23]. Given the high mortality rate associated with RA-ILD, early diagnosis and proactive management are essential. This study revealed that the onset of RA-ILD typically occurs predominantly in patients in their 60s, which is consistent with findings from prior studies [24]. In terms of HRCT manifestations, RA-ILD often presents with a UIP pattern, and previous studies have shown that UIP is a risk factor for mortality in RA-ILD patients [25, 26]. Additionally, the distribution of lesions in the RA group was predominantly subpleural, which may also indicate that UIP is a common pattern. Additionally, this study revealed that bronchiectasis, the absence of esophageal dilation, and a more extensive honeycombing pattern are common HRCT manifestations of RA-ILD. Notably, bronchiectasis and the extent of honeycombing serve as significant predictors, indicating that fibrotic changes that occur in RA-ILD are more severe than those observed in other forms of CTD-ILD. It is worth nothing that this study focused on patients with CTD-ILD that can be definitively classified; however, in the clinic, a subset of patients may present only with interstitial lung abnormalities in the initial phase, and previous studies have shown that 57% of patients with RA-ILA will experience radiographic progression within 1.5 years [27].

The presence of pSjS may be linked to both neoplastic and nonneoplastic proliferation of lymphoid tissues; therefore, greater vigilance is essential for patients with pSjS, particularly those lacking typical clinical symptoms but exhibiting suggestive findings on imaging [28]. HRCT revealed pulmonary abnormalities in 50% of patients with pSjS [29]. In this study, significant HRCT manifestations included enlarged mediastinal lymph nodes, thin-walled cysts, and the absence of esophageal dilation. Logistic regression analysis revealed that mediastinal lymph node enlargement and thin-walled cysts were significant predictors of pSjS. pSjS is a systemic lymphoplasmacytic

infiltrative disease, and it frequently causes enlargement of mediastinal lymph nodes in both the mediastinum and other body regions. However, the clinical significance of mediastinal lymph node enlargement may be ambiguous, potentially indicating systemic lymphoplasmacytic inflammation or mediastinal lymphoma [30]. Additionally, some patients may present with cystic lung lesions, including amyloidosis, pulmonary lymphoma, and LIP [30]. Although LIP is not the most common HRCT manifestation pattern in pSjS, it is recognized to correlate with the condition. Furthermore, the association between LIP and amyloidosis—characterized by multiple irregular nodules on HRCT—is well documented. Given that patients with pSjS are at increased risk of developing pulmonary lymphoma, the presence of LIP alongside multiple nodules on HRCT should prompt the consideration of a neoplastic process [31, 32]. A small review of CT manifestations in five patients with lymphoma (incidental amyloidosis) identified lung nodules of varying sizes and irregularities, as well as multiple cysts [31]. However, this study did not find statistically significant differences in the presence of intrapulmonary nodules among the groups, likely due to the exclusion of patients with pulmonary lymphoma.

In SSc, lung lesions are common and often severely affect organ function; these lesions are characterized primarily by ILD and pulmonary hypertension, which are leading causes of mortality in SSc patients [33]. The most prevalent HRCT pattern observed was NSIP [20]; however, the prevalence of NSIP was not statistically significant in this study, although it was present in 68.8% of SSc-ILD patients, which is consistent with trends observed in previous research. The occurrence of esophageal dilation was found to be statistically significant ($p < 0.001$), which was attributed to the proliferation of submucosal fibrous tissue and atrophy of the muscularis propria in the esophagus. This feature is a more specific manifestation of SSc than other CTD-ILDs. Previous studies have indicated that the prevalence of SSc complicated by pulmonary hypertension is approximately 34.8% [34], representing the highest rates among CTDs. In the present study, 37.5% of patients presented with widened pulmonary trunks, and this is a slightly greater proportion than reported in earlier studies. This discrepancy may have occurred because patients in the present study were not subjected to right-sided heart catheterization for accurate measurements but were classified on the basis of the width of the pulmonary trunks (with widening defined as a pulmonary trunk width of ≥ 29 mm [6]), which is a method that involves a certain degree of error.

In the present study, post hoc tests revealed a significantly earlier age of onset in the PM/DM group than in the RA group, with 56.3% of patients experiencing onset between the ages of 30 and 50 years. Therefore, younger patients with ILD should be aware of the possibility of PM/DM development. PM/DM is the most prevalent type of disease observed in OP, which is consistent with findings from previous studies [3]. Additionally, previous research has shown that lung involvement is rare and much less common in patients with SLE than in those with other CTDs and most often presents as a result of plasmapheresis [3]. In this study, 50% of the SLE patients were found to have pericardial effusion, and 16.7% had pleural effusion. However, owing to the small sample size of SLE patients, these findings did not reach statistical significance.

In this study, among the CTD-ILD groups with honeycombing as the primary manifestation, RA was the most common, and this group had a greater extent of honeycombing. This finding indicates that RA is associated with more severe fibrosis, further confirming that UIP is the most prevalent HRCT manifestation of RA-ILD. The predominant manifestation of reticulation is more commonly observed in PM/DM patients and less commonly in RA patients, whereas consolidation is the predominant manifestation that is more frequently observed in PM/DM patients. However, no statistically significant difference was found in the extent of reticulation or consolidation. In this study, we did not utilize the traditional five-step method [35] to score the extent of lesions; instead, we precisely quantified the lesion extent through quantitative CT analysis of multiple ROIs. By combining visual assessment with quantitative CT, we leveraged the extensive experience and knowledge of clinicians to identify signs that may not be quantifiable as well as other systemic chest signs, such as esophageal dilation. Objective and standardized measurements were performed via advanced image analysis software for those aspects suitable for quantification, aiming to explore valuable predictive indices in CTD-ILD.

This study has several limitations. First, this was a retrospective study, the clinical diagnoses relied on multidisciplinary consultations, and there was a lack of pathological evidence. Second, the sample size of this study was small, and logistic regression analysis was not performed for the SSc, PM/DM, and SLE groups, which limited the ability to generate significant predictive indices.

Conclusion

The presence of bronchiectasis and extensive honeycombing were significant in the RA group, indicating a more severe degree of fibrosis compared with the other groups, and fibrosis primarily was characterized by a honeycomb pattern. The presence of thin-walled cysts and enlarged mediastinal lymph nodes in the pSjS group were significant predictors, highlighting the distinctive pattern of LIP and the proliferation of lymphoid tissues

in patients with pSjS. Esophageal dilatation was a characteristic feature in the SSc group, distinguishing it from other CTD-ILD types. Compared with the other groups, the PM/DM group had a younger age of onset, with OP being its distinctive pattern. Owing to these characteristic findings, the combined assessment of visual methods and quantitative CT analysis is clinically relevant for the accurate diagnosis of different types of CTD-ILD.

Abbreviations

CTD	Connective tissue diseases
ILD	Interstitial lung disease
CTD-ILD	Connective tissue disease-associated interstitial lung disease
RA	Rheumatoid Arthritis
RA-ILD	Rheumatoid arthritis-related interstitial lung disease
pSjS	Primary Sjögren's syndrome
pSjS-ILD	Primary Sjögren's syndrome-related interstitiallung disease
SSc	Systemic Sclerosis
SSc-ILD	Systemic Sclerosis-related interstitial lung disease
PM/DM	Polymyositis/dermatomyositis
PM/DM-ILD	Polymyositis/dermatomyositis-related interstitial lung disease
SLE	Systemic Lupus Erythematosus
SLE-ILD	Systemic lupus erythematosus-related interstitial lung disease
HRCT	High Resolution Computed Tomography
UIP	Usual interstitial pneumonia
NSIP	Nonspecific interstitial pneumonia
LIP	Lymphocytic interstitial pneumonia
OP	Organizing pneumonia
IIP	Idiopathic interstitial pneumonia
EULAR	European League Against Rheumatism
ROI	Region of interest
95%CI	95% Confidence Interval

Acknowledgements
All authors would like to thank all healthcare workers who contributed to this study.

Author contributions
X.L. X.Z. and X.Z. were responsible for collecting cases, and G.W. evaluated the image. X.L. and H.Z. were responsible for image processing and ROI delineation, X.L. written the manuscript, and J.Z. rigorously revised the manuscript.

Funding
Beijing Kanghua Traditional Chinese and Western Medicine Development Foundation (No. KH–2022–DXJJ–022).

Data availability
The data underlying this study may be made available upon reasonable request to the corresponding authors.

Declarations

Ethics approval and consent to participate
The study was conducted in accordance with the Declaration of Helsinki and informed consent was secured from all participants. This study had been approved by the ethics committee of the Second Affiliated Hospital of Harbin Medical University (Ethics No. YJSKY2024-057).

Consent for publication
Not applicable.

Competing interests
The authors declare no competing interests.

Received: 5 December 2024 / Accepted: 31 March 2025
Published online: 07 April 2025

References

1. Homma Y, Ohtsuka Y, Tanimura K, et al. Can interstitial pneumonia as the sole presentation of collagen vascular diseases be differentiated from idiopathic interstitial pneumonia? Respiration. 1995;62(5):248–51.
2. Travis WD, Costabel U, Hansell DM, et al. An official American thoracic society/European respiratory society statement: update of the international multidisciplinary classification of the idiopathic interstitial pneumonias. Am J Respir Crit Care Med. 2013;188(6):733–48.
3. Elicker BM, Kallianos KG, Henry TS. Imaging of the thoracic manifestations of connective tissuedisease. clin. Chest Med. 2019;40(3):655–66.
4. Joy GM, Arbiv OA, Wong CK, et al. Prevalence, imaging patterns and risk factors of interstitial lung disease in connective tissue disease: a systematic review and meta-analysis. Eur Respir Rev. 2023;32(167):220210.
5. Chen A, Karwoski RA, Gierada DS, Bartholmai BJ, Koo CW. Quantitative CT analysis of diffuse lung disease. Radiographics. 2020;40(1):28–43.
6. Tan RT, Kuzo R, Goodman LR, Siegel R, Haasler GB, Presberg KW. Utility of CT scan evaluation for predicting pulmonary hypertension in patients with parenchymal lung disease. Medical college of Wisconsin lung transplant group. Chest. 1998;113(5):1250–6.
7. Colak S, Tekgoz E, Gunes EC, et al. Clinical characteristics of patients with connective tissue disease-related interstitial lung disease: a retrospective analysis. Clin Rheumatol. 2024;43(5):1693–701.
8. Hsu E, Shi H, Jordan RM, Lyons-Weiler J, Pilewski JM, Feghali-Bostwick CA. Lung tissues in patients with systemic sclerosis have gene expression patterns unique to pulmonary fibrosis and pulmonary hypertension. Arthritis Rheum. 2011;63(3):783–94.
9. Peljto AL, Steele MP, Fingerlin TE, et al. The pulmonary fibrosis-associated MUC5B promoter polymorphism does not influence the development of interstitial pneumonia in systemic sclerosis. Chest. 2012;142(6):1584–8.
10. Hant FN, Ludwicka-Bradley A, Wang HJ, et al. Surfactant protein D and KL-6 as serum biomarkers of interstitial lung disease in patients with scleroderma. J Rheumatol. 2009;36(4):773–80.
11. Ytterberg AJ, Joshua V, Reynisdottir G, et al. Shared immunological targets in the lungs and joints of patients with rheumatoid arthritis: identification and validation. Ann Rheum Dis. 2015;74(9):1772–7.
12. Atzeni F, Gerardi MC, Barilaro G, Masala IF, Benucci M, Sarzi-Puttini P. Interstitial lung disease in systemic autoimmune rheumatic diseases: a comprehensive review. Expert Rev Clin Immunol. 2018;14(1):69–82.
13. Lynch DA. Lung disease related to collagen vascular disease. J Thorac Imaging. 2009;24(4):299–309.
14. Tanizawa K, Handa T, Nakashima R, et al. HRCT features of interstitial lung disease in dermatomyositis with anti-CADM-140 antibody. Respir Med. 2011;105(9):1380–7.
15. Won Huh J, Soon Kim D, Keun Lee C, et al. Two distinct clinical types of interstitial lung disease associated with polymyositis-dermatomyositis. Respir Med. 2007;101(8):1761–9.
16. Teixeira L, Mouthon L, Mahr A, et al. Mortality and risk factors of scleroderma renal crisis: a French retrospective study of 50 patients. Ann Rheum Dis. 2008;67(1):110–6.
17. Tansey D, Wells AU, Colby TV, et al. Variations in histological patterns of interstitial pneumonia between connective tissue disorders and their relationship to prognosis. Histopathology. 2004;44(6):585–96.
18. Tanaka N, Kunihiro Y, Kubo M, et al. HRCT findings of collagen vascular disease-related interstitial pneumonia (CVD-IP): a comparative study among individual underlying diseases. Clin Radiol. 2018;73(9):e8331–83310.
19. Silva CI, Müller NL. Interstitial lung disease in the setting of collagen vascular disease. Semin Roentgenol. 2010;45(1):22–8.
20. Giacomelli R, Liakouli V, Berardicurti O, et al. Interstitial lung disease in systemic sclerosis: current and future treatment. Rheumatol Int. 2017;37(6):853–63.
21. Samhouri BF, Vassallo R, Achenbach SJ, et al. Incidence, risk factors, and mortality of clinical and subclinical rheumatoid Arthritis-Associated interstitial lung disease: A Population-Based cohort. Arthritis Care Res (Hoboken). 2022;74(12):2042–9.
22. Young A, Koduri G, Batley M, et al. Mortality in rheumatoid arthritis. Increased in the early course of disease, in ischaemic heart disease and in pulmonary fibrosis. Rheumatology (Oxford). 2007;46(2):350–7.
23. Kelly CA, Saravanan V, Nisar M, et al. Rheumatoid arthritis-related interstitial lung disease: associations, prognostic factors and physiological and radiological characteristics–a large multicentre UK study. Rheumatology (Oxford). 2014;53(9):1676–82.

24. Kim EJ, Collard HR, King TE Jr. Rheumatoid arthritis-associated interstitial lung disease: the relevance of histopathologic and radiographic pattern. Chest. 2009;136(5):1397–405.
25. Qiu M, Jiang J, Nian X, et al. Factors associated with mortality in rheumatoid arthritis-associated interstitial lung disease: a systematic review and meta-analysis. Respir Res. 2021;22(1):264.
26. Nieto MA, Rodriguez-Nieto MJ, Sanchez-Pernaute O, et al. Mortality rate in rheumatoid arthritis-related interstitial lung disease: the role of radiographic patterns. BMC Pulm Med. 2021;21(1):205.
27. Gochuico BR, Avila NA, Chow CK, et al. Progressive preclinical interstitial lung disease in rheumatoid arthritis. Arch Intern Med. 2008;168(2):159–66.
28. Woodhead F, Wells AU, Desai SR. Pulmonary complications of connective tissue diseases. Clin Chest Med. 2008;29(1):149–vii.
29. Matsuyama N, Ashizawa K, Okimoto T, Kadota J, Amano H, Hayashi K. Pulmonary lesions associated with Sjögren's syndrome: radiographic and CT findings. Br J Radiol. 2003;76(912):880–4.
30. Luppi F, Sebastiani M, Sverzellati N, Cavazza A, Salvarani C, Manfredi A. Lung complications of Sjogren syndrome. Eur Respir Rev. 2020;29(157):200021.
31. Jeong YJ, Lee KS, Chung MP, et al. Amyloidosis and lymphoproliferative disease in Sjögren syndrome: thin-section computed tomography findings and histopathologic comparisons. J Comput Assist Tomogr. 2004;28(6):776–81.
32. Masaki Y, Sugai S. Lymphoproliferative disorders in Sjögren's syndrome. Autoimmun Rev. 2004;3(3):175–82.
33. Chaisson NF, Hassoun PM. Systemic sclerosis-associated pulmonary arterial hypertension. Chest. 2013;144(4):1346–56.
34. Chung L, Liu J, Parsons L, et al. Characterization of connective tissue disease-associatedpulmonary arterial hypertension from REVEAL: identifying systemic sclerosis as a unique phenotype. Chest. 2010;138(6):1383–94.
35. Park WH, Kim SS, Shim SC, et al. Visual assessment of chest computed tomography findings in Anti-cyclic citrullinated peptide antibody positive rheumatoid arthritis: is it associated with airway. Abnormalities? Lung. 2016;194(1):97–105.

Publisher's note